We are IntechOpen, the world's leading publisher of Open Access books Built by scientists, for scientists

6,900
Open access books available

186,000
International authors and editors

200M
Downloads

Our authors are among the

154
Countries delivered to

TOP 1%
most cited scientists

12.2%
Contributors from top 500 universities

WEB OF SCIENCE™

Selection of our books indexed in the Book Citation Index in Web of Science™ Core Collection (BKCI)

Interested in publishing with us?
Contact book.department@intechopen.com

Numbers displayed above are based on latest data collected.
For more information visit www.intechopen.com

11

Microfinite Element Modelling for Evaluating Polymer Scaffolds Architecture and their Mechanical Properties from Microcomputed Tomography

Angel Alberich-Bayarri[1], Manuel Salmerón Sánchez[2]
M. Ángeles Pérez[3] and David Moratal[2]
[1] *Department of Radiology, Hospital Quirón Valencia, Valencia, Spain.*
[2] *Center for Biomaterials and Tissue Engineering, Universitat Politècnica de València, Valencia, Spain.*
[3] *Group of Structural Mechanics and Materials Modeling, Instituto de Investigación en Ingeniería de Aragón, Universidad de Zaragoza, Zaragoza, Spain.*

1. Introduction

With increasing time of life expectation, problems related to bone loss are one of the major causes of disability. Nowadays, the current standard therapy for treating bone atrophy consists on bone allografts and autografts (Rajan et al., 2006). Metal implants have also been used for the assessment of bone defects. These therapies present some drawbacks, allografts and autografts are limited by availability of material, donor site morbidity and also the possibility of disease transmission or immune rejection in the case of allografts (Geffre et al., 2009). In the case of metal implants, a high availability exists and also the risk of transmittable diseases from donor to host is eliminated. However, additional surgeries can be needed due to complications related with stress shielding, infection or implant failure.

In the last decades, there has been a growing interest in polymer scaffolds which encourage bone regeneration to treat bone defects (Parson, 1985). These scaffolds can be prepared prior to or during surgery, can be modified to alter mechanical strength and resorption rate, can be created in custom shapes unique to each defect site, and can be produced with highly controlled structures (Geffre et al., 2009).

Polymer scaffolds of different architectures are commonly synthesized with the main objective of obtaining effective functional biological responses. Such structures are designed to behave as an extracellular matrix where cells organize into a three dimensional architecture, stimulating the growth of new tissue (Langer & Vacanti, 1993; Hutmacher 2000; Freed et al., 1998; Yang et al., 2001).

Tissue engineering techniques are focused on the design of scaffolds that match biological and physio-chemical properties of the tissue where they are settled. In the case of bone, the bone is formed by osteoblasts that migrate from the adjacent original bone and marrow

cavities, a mechanism known as osteoconduction. Although this osteointegration is mandatory, there are situations (e.g., large defects) where the scaffolds not only are designed to provide the template for tissue regeneration but also need to be osteinductive, that is, stimulate the migration of undifferentiated cells and induce their differentiation into active osteoblasts in order to boost de young bone formation (Oliveira et al., 2009). In order to improve the growth stimulating properties of grafting materials, they have been combined with growth factors and different cells types with variable results depending on the host regenerative capability (Dupraz et al., 1998; Gauthier et al., 2003).

Several methods have been developed for 3D polymer scaffold synthesis with different resultant structure properties regarding network topology, pores shape and density, determining their biological and mechanical functional response (Gao et al., 2003; Horbett et al., 1985; Zhang & Ma, 1999). The different methods used for scaffolds synthesis define the final 3D architecture. The most common techniques for fabric preparation are porogen leaching (Mikos et al., 1993; Zhou et al., 2005), fibre templates (Thomson et al., 1995), phase separation (Gao et al., 2003), emulsion freeze-drying (Whang et al., 1995), gas foaming (Harris et al., 1993), and solid free fabrication (SFF)-rapid prototyping (RP) techniques (Moroni et al., 2006). However, the control of these synthesized scaffold characteristics in the fabrication process is still the hobbyhorse of this science (Freed et al., 1998; Yang et al., 2001; Hajiali et al., 2010).

The architecture of scaffolds can be evaluated after the fabrication process by different ways. Although there are several techniques for scaffold analysis, a reasonable classification is based on the destructive or non-destructive nature of the methodology. Destructive methods are those in which the sample under analysis is deteriorated and is no longer useful to perform more measurements. The compressive stress-strain measurements using a load cell are performed experimentally and are an example of destructive methodology. An ideal way to evaluate the scaffold 3D structural design after the fabrication process would consist on a non-destructive, non-invasive and quantitative technique. In this sense, the use of micro-computed tomography (μCT) scanners have allowed for the non-destructive and non-invasive examination of scaffolds at a high spatial resolution (Ho & Hutmacher, 2006). The use of μCT has also eased the quality control of scaffold fabrication processes, the study of scaffold degradation kinetics and the assessment of bone tissue response (van Lenthe et al., 2007). Even more, the recent application of advanced image processing algorithms and simulation-based computational methods, like the Finite Element (FE) method to micro-computed tomography (μCT) acquisitions, have allowed for the texture and virtual mechanical analysis of different scaffold 3D architectures (Alberich-Bayarri et al., 2009).

The combination of the FE method with μCT acquisitions (also called μFE) and image processing techniques as an alternative instrument for the mechanical properties evaluation of synthetic scaffolds is very recommendable. The geometrical fidelity of the corresponding structure to be analyzed by FE is a very important issue. This geometrical modelling can be obtained with high detail and reliability from μCT scans. The combination of μCT reconstructions and FE analysis for scaffolds design has been widely investigated in the literature. In this sense, a relevant study characterized porous phosphate glass and macroporous calcium phosphate bone cement, initially using μCT to investigate the porosity and then through the μFE method for the stress-strain analysis and influence of the cells attached to the material (Lacroix et al., 2006). A published work also described a μCT based FE modelling of native trabecular bone and bone scaffolds (Jaecques et al., 2004).

In this chapter, the process for a non-invasive analysis of synthetic polymer scaffolds using the μCT acquisition technique in combination with the μFE method is extensively described. Some results and examples of the application of the methodology to different scaffold architectures are exposed. Finally, the elasticity modulus results obtained in different scaffold architecture are compared to the obtained experimentally in the corresponding stress-strain essays.

2. Image acquisition and processing

Polymer scaffold characteristics can be obtained after proper image processing from micro-computed tomography images (μCT). The μCT technique serves to analyze the inner 3D architecture of an object by image analysis. The sample is irradiated with X-rays in a series of 2D slices. The radiation attenuates while crossing the slice and arrives at the detectors with a reduced energy. Then, the corresponding attenuation coefficients can be calculated. These coefficients are directly related to the density of the materials forming the sample. An image is finally calculated with pixel intensities scaled by the densities of the materials forming the sample (Ho & Hutmacher, 2006).
The μCT is a scanning system that is much higher in resolution than conventional clinical scanners. Clinical tomographic scanners may have resolutions on the order of half a millimetre or less. However, μCT scanners permit the acquisition at very high spatial resolutions. In concrete, actual μCT scanners allow spatial resolutions of a few micrometers down to even nanometers if the proper technology is available. With the significant increase in μCT spatial resolution, there is also an associated decrease in imaging field of view. This is the reason that explains the limitation and use of these scanners to research areas for the analysis of biopsied biological tissue, different materials or small samples.

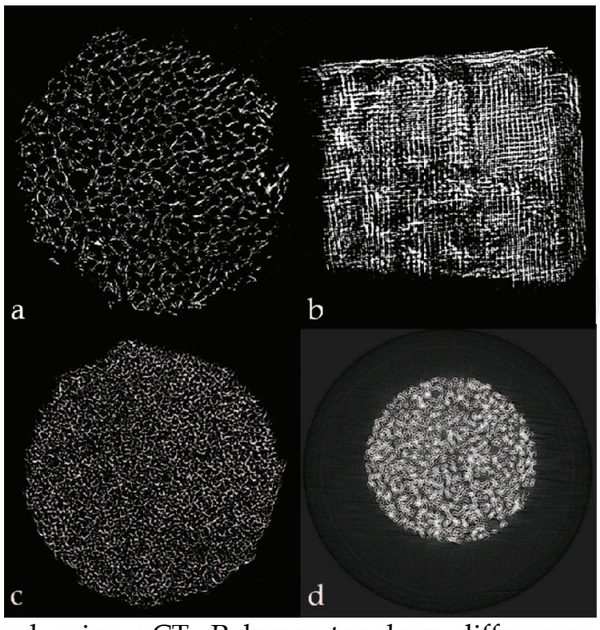

Fig. 1. Images acquired using μCT. Polymer topology differences may be appreciated. Spherical pores structure was synthesized in scaffolds a), c) and d) while an orthogonal pore mesh is shown in b).

In the process of scaffold analysis, the first step is the μCT acquisition. In order to explain the methodology of processing and analysis with a practical case, scaffolds of different synthesized topologies (spherical pores, cylindrical orthogonal pore mesh, salt particles) were scanned using a μCT system (SkyScan, Kontich, Belgium). A set of 2D slices covering the entire sample were obtained. A very high isotropic spatial resolution of 7μm was achieved in acquisition. Representative slices of the μCT images acquired from different scaffolds are shown in figure 1.

Some pre-processing is required after acquisition. First of all, volumes of interest (VOI) are extracted semi-automatically from each dataset. The process consists on initially defining a squared region of interest (ROI) placed in one of the slices of the dataset, the ROI must be inscribed in the circle defined by the cylindrical section of the scaffold (as it can be observed in figure 2-a). Then, the ROI is propagated through the rest of the slices, verifying that the selected volume exclusively contains inner structural data and not surrounding air. A new dataset is created with the segmented region of each slice (figure 2-b).

After segmentation, structure voxels must be differentiated from pore voxels, that is, images must be converted to its binarized form. The thresholding is implemented in a slice by slice basis by means of the Otsu's method (figure 2-c) (Otsu, 1979). As a result, a three-dimensional (3D) binary matrix representing the segmented volume of polymer under study is obtained.

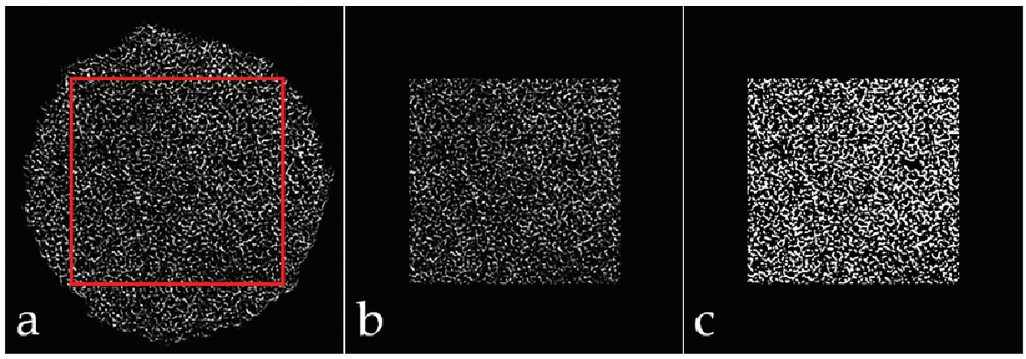

Fig. 2. In a), example of the definition of the inscribed ROI to be propagated through the rest of the slices for the VOI segmentation. In b), new dataset creation with the segmented ROI's for each slice. In c), binary image resulting from the thresholding process applied to the segmented dataset.

3. Volumetric reconstruction and meshing

Once the region under analysis has been binarized, the resulting 3D logical matrix can be visualized by a volumetric reconstruction process. An initial smoothing is performed to the volume in a 3D routine and then, the marching cubes algorithm (Lorensen & Cline, 1987) is applied in order to obtain a volumetric reconstruction of the scaffold structure, as it can be seen in figure 3 for the different scaffold topology.

In order to build the μFE mesh from the volumetric data of the 3D binary matrix, the voxels corresponding to polymer must be converted to very small structural elements with certain coordinates and dimensions. There are different types of elements for FE volumetric modelling, like tetrahedrons or hexahedrons. In our case, the element used to form the mesh

is an eight-noded hexahedron, also called 'brick' element. However, the meshing process is not trivial and it supposes a high computational cost. To convert the volumetric reconstructions to a μFE mesh, a fast voxel mesher specially designed for this application is applied (Alberich-Bayarri et al., 2007). The meshed scaffolds have a mean number of 3000000 nodes and 1400000 elements, approximately.
After both nodes and elements lists are defined, they must be converted to a format that can be interpreted by common FE simulation software, like ANSYS (Ansys Inc., Southpointe, PA, USA) or ABAQUS (Simulia, Providence, RI, USA). To do that, a specially designed routine translates the raw data into standardized *.ans, for ANSYS or *.inp for ABAQUS FE analysis software.

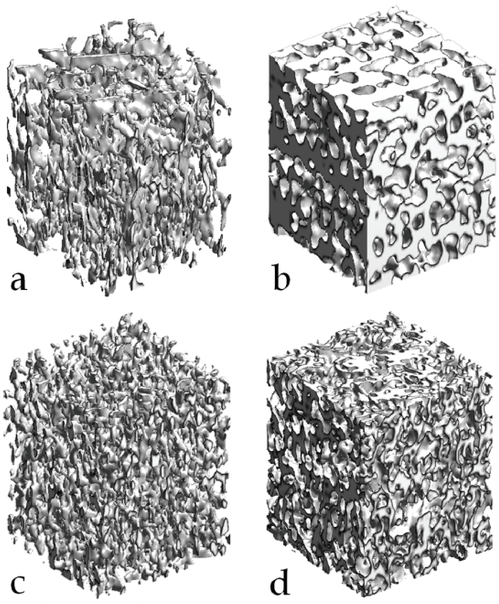

Fig. 3. 3D reconstructions of the different scaffolds after segmentation and thresholding. Same topologies distribution than in figure 1. Spherical pores in a), c) and d); orthogonal pore mesh in b).

Finally, the mesh can be loaded in the corresponding FE analysis platform (figure 4).

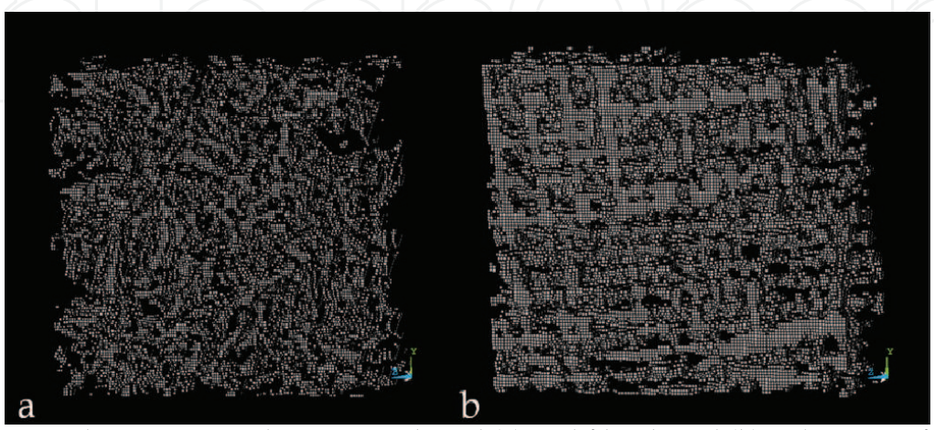

Fig. 4. μFE meshes corresponding to pore based (a) and fiber based (b) polymer scaffolds.

4. FE model definition

Once the mesh is loaded, the model has to be defined by the specification of the material properties, the boundary conditions and the specific essay to be simulated. Regarding the material properties, each element is assigned linear elastic isotropic properties consisting of a bulk elasticity modulus of Eb=1MPa and a Poisson's ratio v=0.3.

The aim of the process is to simulate a compressive stress-strain test of the scaffold. To specify this situation, first, boundary conditions must be defined. A null displacement in the three directions of space is imposed on nodes from one side of the sample. Thus, this side remains fixed when any load is applied to the structure. After definition of boundary conditions, the situation required to simulate compression needs to be specified. Thus, a deformation of 10% of the scaffold edge length is imposed on nodes from the opposite side.

5. Simulation and results calculation

Simulations of the generated μFE models are performed by the application of the generalized structural mechanics theory (Zienkiewicz et al., 2006) to the system of equations defined by the previously imposed conditions. The mathematical steps for the solution calculation are widely explained in chapter "*Finite Element Modeling for a Morphometric and Mechanical Characterization of Trabecular Bone from High Resolution Magnetic Resonance Imaging*" of this book.

In practice, the solution is calculated in efficient software platforms specially designed for large array processing. The identification of one element to each voxel supposes a high computational burden, especially when the number of nodes tends to be greater than $1x10^6$, due to the large stiffness matrices to be assembled and the significant increase in the degrees of freedom. There are three degrees of freedom per node and each element has 8 nodes (24 equations per element). Different methods may be used for solving these large systems of differential equations. In our case, as mentioned in chapter about FE analysis of trabecular bone of this book, for trabecular bone simulations, systems are solved by Gaussian elimination using a standard sparse solver. All the nodal forces and displacements of the structure are obtained and the nodal stresses and strains can be calculated. In addition, the elastic modulus of the porous structure (E) can be efficiently estimated by the homogenization theory approximation, based on linear elastic behaviour and small deformations theory (Hollister et al., 1991; Hollister & Kikuchi, 1992).

The different solutions can be represented in a parametric 3D reconstruction in order to graphically evaluate regions with certain mechanical conditions. If a compressive essay is simulated in the different scaffolds shown in figures 1 and 2, it is observed that the normal stress distributions are not similar between the different architectures. In this sense, Figure 5a-c shows that the scaffolds with spherical pores have a uniform stress distribution and pores do not act as stress concentrators as it would happen if only one of spherical pore were surrounded by the scaffolding material (Alberich-Bayarri et al., 2009). However, stress tends to concentrate around the channels of the scaffold with crossed fibers, as it can be observed in figure 5b. This could be explained by the inherent anisotropy of the scaffold and by the lower porosity in comparison to spherical pores scaffolds.

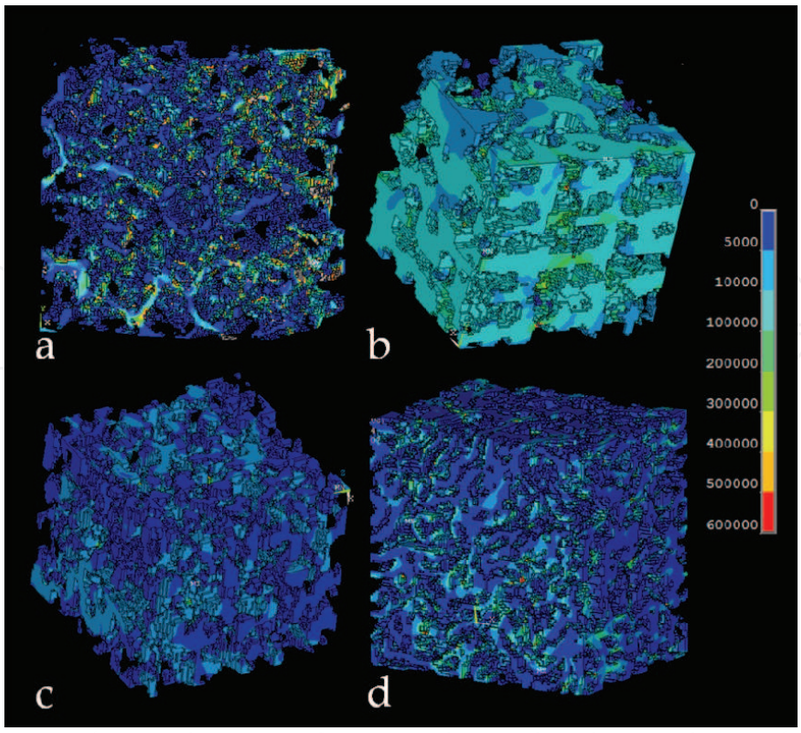

Fig. 5. Distribution of normal stresses. Same topologies distribution than in figures 1 and 2. Spherical pores in a), c) and d); orthogonal pore mesh in b).

Results can be quantitatively compared between different architectures. Table 1 shows the stresses and Young's modulus obtained with μFE. It can be observed that the scaffold based on crossed channels (which corresponds to Figure 5-b) shows a high maximum stress and apparent Young's modulus in comparison to other topologies.

	PLLA (salt particles)	PMMA (sphere porogens)	Fiber templates
S_{MAX} [MPa]	0,82	0,83	1,02
E_{app} [kPa]	2.53	19.99	152.44

Table 1. Maximum stresses and apparent Young's modulus obtained for three different scaffold architectures (Poly-L-Lactide Acid, PLLA; Poly(methyl methacrylate), PMMA; fiber templates).

If the results obtained for the apparent Young's modulus parameter are compared to structure porosity, that can be directly calculated from the 3D reconstructions, it is appreciated that a dependence of the normalized modulus (to the bulk) with the square of porosity exists. Both the experimental measurements and the μFE results are well correlated with the proposed exponential dependence for the compressive modulus on porosity (Gibson & Ashby,2001), as it can be observed in figure 6.

$$\frac{E_{app}}{E_b} = C\left(\frac{\rho}{\rho_b}\right)^2 \quad (1)$$

Where ρ and ρ_b are the apparent density of the scaffold and bulk density of the constituting material, respectively.

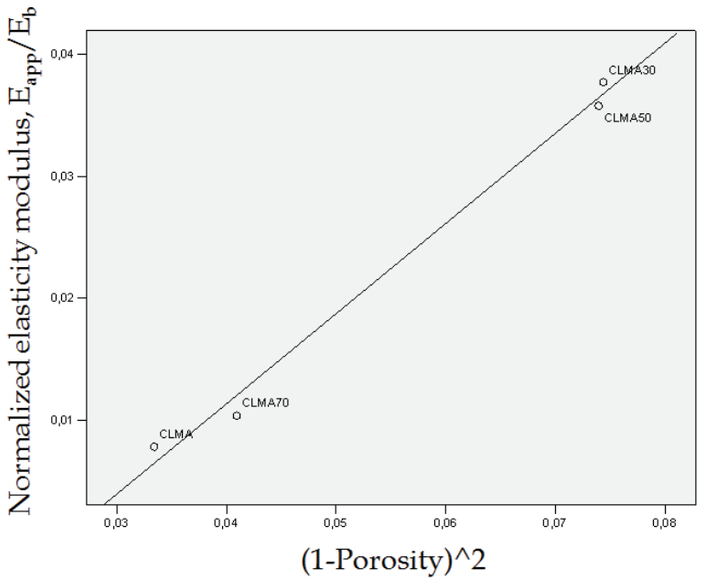

Fig. 6. Relationship (r^2=0.92) between normalized Young's modulus and the square of porosity in four different PMMA scaffolds analyzed.

The existence of a general relationship (in the elastic regime) between the modulus and porosity is evidenced with the analysis of these results. This has been also suggested in previous works in which interconnected spherical pores of different sizes and interconnected throats have been investigated (Diego et al., 2007). Even more, a similar behaviour was observed for Young's modulus analysis of trabecular bone in a population of healthy patients (Alberich-Bayarri et al., 2008; Gibson & Ashby, 2001).

6. Validation with experimental measurements

The μFE simulations and measurements are performed in a non-destructive way, that is, mechanical properties are extracted without compromising the structure to real mechanical loads. Although the FE methods have been widely extended and are essential in any engineering process because of their accuracy and reliability, the last affirmation is relatively ambitious and the indirect measurements performed by FE method need to be validated with the standard reference technique, that is, with experimental compression stress-strain measurements. This technique performs a continuous sampling of the stress-strain relationship during the essay to obtain curves showing the mechanical behaviour of the specimen being analyzed. An example of a real stress-strain curve can be observed in figure 7.

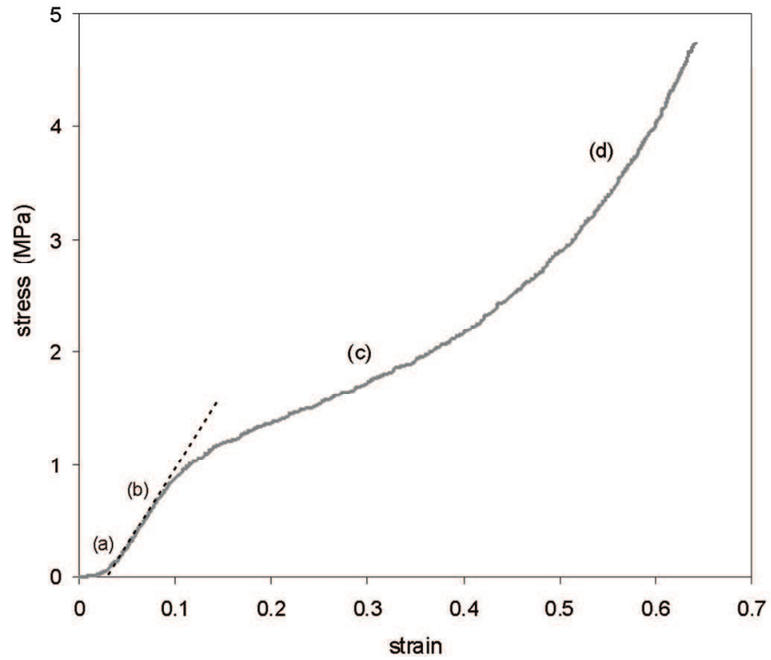

Fig. 7. Experimental stress–strain curve of a scaffold with interconnected spherical pores. The letters on the curve are related to different mechanical features. Briefly: (a) contact region between the sample and the device; (b) the linear elastic region (the elastic modulus was calculated from the slope of the dotted line); (c) buckling phenomenon leading to the so-called plateau; and (d) final collapse of the structure increasing the compressive modulus. (Adapted from Alberich-Bayarri et al., 2009).

In order to evaluate the measurements of scaffolds Young's modulus, the measurements performed in two different scaffolds topologies (interconnected spherical pores, crossed fibers) using both μFE and experimental techniques were compared. Experimental compression stress-strain measurements were performed on a Microtest system with a load cell of 15N. The samples consisted on cylinders with an approximated radius of 5mm and 3mm height. The initial range of strains (0–0.1) was underestimated due to the non-conformity of the contact between the machine plate and the specimen. Thus, the experimental compressive modulus of the scaffold was not easy to measure. The test was carried out until microstructure was completely collapsed. Finally, the compressive modulus was determined from the initial linear slope of the curve after full contact between plate and specimen was ensured.

In figure 8, the mentioned dependence of the normalized modulus (to the bulk) as a function of the square of porosity can be observed. The μFE and the experimental results can be also compared. Both methods are accomplishing the proposed exponential relationship between the compressive modulus and scaffold porosity. The effectiveness of the μFE method used for the calculation of mechanical characteristics is demonstrated. The obtained values of elasticity modulus by the μFE method are well related to those obtained experimentally. The agreement between the experimental results and the μFE simulations supports the feasibility of the technique as a tool for scaffold design and non-invasive analysis on real fabricated scaffolds before physical experiments are planned.

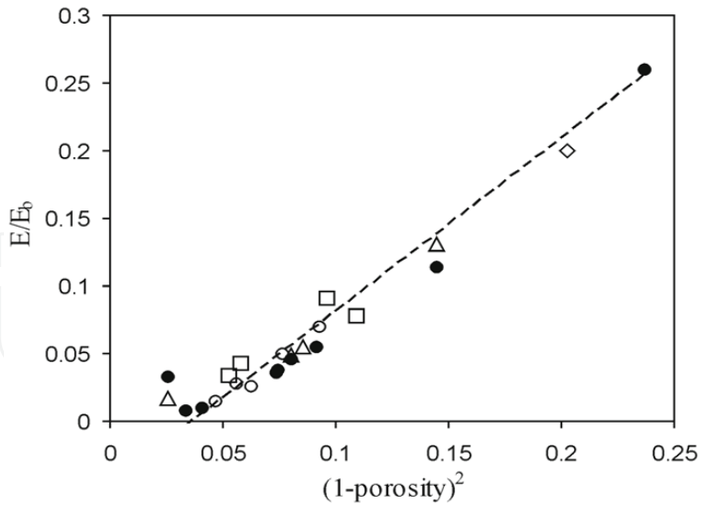

Fig. 8. μFE calculated (black dots) and experimentally measured normalized (to the bulk Eb) moduli for the different structures: (squares) constructs with spherical pores, (diamonds) construct with orthogonal cylindrical pores, (delta) construct based on salt particles. Additional points (circle) from (Diego et al. 2007) have been included so as to reinforce the universality of the relationship between the (reduced) elastic modulus and porosity. (Adapted from Alberich-Bayarri et al., 2009).

7. Conclusions and future challenges

During the last decades, treatment of bone defects has been directed to the research in polymer scaffolds of different architectures. Scaffolds play a key role in bone regeneration and the design of their 3D architecture is crucial to develop their function.

The use of high spatial resolution acquisitions from μCT scanners in combination with advanced image processing methods represent a powerful tool to develop a structural and mechanical characterization of the synthesized polymer scaffolds and evaluate the achievement of the desired properties at the manufacture stage.

The algorithms employed for the image analysis and fast meshing processes allows for the detailed numerical simulations of the mechanical properties at a micro scale level, also called μFE. These simulations suppose a high computational burden that can be optimized by proper μFE model definition. μFE results obtained for the apparent Young's modulus are highly close to the experimental results.

All the simulations performed in the synthesized scaffolds using the μFE method have been done in the linear behaviour domain. However, in future it would be of high interest to improve in the knowledge of the non-linear behaviour of the scaffolds when strong compressive conditions are considered and buckling processes begin.

Also, the analysis of the scaffolds using μCT combined with μFE before and after cell seeding would help to evaluate the non-invasive method proposed as a reliable way to quantify the levels of new tissue deposition in the scaffold.

Acknowledgements

The support of the Spanish Ministry of Science and Innovation through project TEC2009-14128 and of the Generalitat Valenciana through projects GV/2009/126 (grups d'investigació emergents) and ACOMP/2010/022 (ajudes complementàries) is acknowledged.

The authors like to thank the 3B's Research Group-Biomaterials, Biodegradables and Biomimetics of the University of Minho (Braga, Portugal) for the µCT acquisitions.

8. References

Alberich-Bayarri, A.; Moratal, D.; Martí-Bonmatí, L.; Salmerón-Sánchez, M.; Vallés-Lluch, A.; Nieto-Charques, L. & Rieta JJ. (2007). Volume mesh generation and finite element analysis of trabecular bone magnetic resonance images. *Proceedings of: Annual International Conference of the IEEE Engineering in Medicine and Biology Society,* pp. 1603-1606, 1557-170X, Lyon, France, August 2007, *IEEE Engineering in Medicine and Biology Society*.

Alberich-Bayarri, A.; Marti-Bonmati, L.; Sanz-Requena, R.; Belloch, E. & Moratal, D. (2008). In vivo trabecular bone morphologic and mechanical relationship using high-resolution 3-T MRI. *American Journal of Roentgenology,* 191, 3, (Sep 2008), 721-726, 0361-803X.

Alberich-Bayarri, A.; Moratal, D.; Ivirico, J.L.; Rodríguez Hernández, J.C.; Vallés-Lluch, A.; Martí-Bonmatí, L.; Estellés, J.M.; Mano, J.F.; Pradas, M.M.; Ribelles, J.L. & Salmerón-Sánchez, M. (2009). Microcomputed tomography and microfinite element modeling for evaluating polymer scaffolds architecture and their mechanical properties. *Journal of biomedical materials research. Part B, Applied biomaterials,* 91, 1, (Oct 2009), 191-202, 1552-4973.

Diego, R. B.; Estelles, J. M.; Sanz, J. A.; García-Aznar, J. M. & Sánchez, M. S.. (2007). Polymer scaffolds with interconnected spherical pores and controlled arquitecture for tissue engineering: fabrication, mechanical properties and finite element modeling. *Journal of biomedical materials research. Part B, Applied biomaterials,* 81, 2 (May 2007), 448–455, 1552-4973.

Dupraz, A.; Delecrin, J.; Moreau, A.; Pilet, P. & Passuti, N. (1998). Long-term bone response to particulate injectable ceramic. *Journal of biomedical materials research,* 42, 3 (Dec 1998), 368-375, 0021-9304.

Freed, L.E.; Hollander, A.P.; Martin, I.; Barry, L.R. & Vunjak-Novakovic, G. (1998). Chondrogenesis in a cell-polymer-bioreactor system. *Experimental cell research* , 240, 1 (Apr 1998), 58-65, 0014-4827.

Gao, C.Y.; Wang, D.Y. & Shen, J.C. (2003). Fabrication of porous collagen/chitosan scaffolds with controlling microstructure for dermal equivalent. *Polymers for advanced technologies*, 14, 6 (May 2003), 373-379, 1042-7147.

Gauthier, O.; Khairoun, I.; Bosco, J.; Obadia, L.; Bourges, X.; Rau, C.; Magne, D.; Bouler, J.M.; Aguado, E. & Daculsi, G. (2003). Noninvasive bone replacement with a new injectable calcium phosphate biomaterial. *Journal of biomedical materials research. Part A*, 66, 1 (Jul 2003), 47-54, 1549-3296.

Geffre, C.P.; Margolis, D.S.; Ruth, J.T.; DeYoung, D.W.; Tellis, B.C. & Szivek, J.A. (2009). A Novel Biomimetic Polymer Scaffold Design Enhances Bone Ingrowth. *Journal of biomedical materials research. Part A*, 91, 3 (Dec 2009), 795–805, 1549-3296.

Gibson, L.J. & Ashby M. (2001). The mechanics of foam: Basic results. In: *Cellular Solids: Structure and Properties*, Clarke, D.R.; Suresh, S. & Ward, I.M., 175-234, Cambridge University Press, 0521499119, Cambridge, UK.

Hajiali, H.; Karbasi, S.; Hosseinalipour, M. & Rezaie, H.R. (2010). Preparation of a novel biodegradable nanocomposite scaffold based on poly (3-hydroxybutyrate)/bioglass nanoparticles for bone tissue engineering. *Journal of Materials Science. Materials in Medicine*, 2010. [Epub ahead of print], 0957-4530.

Harris, L.D.; Kim, B.S. & Mooney, D.J. (1998). Open pore biodegradable matrices formed with gas foaming. *Journal of biomedical materials research,* 42, 3, (Dec 1998), 396-402, 0021-9304.

Ho, S.T. & Hutmacher, D.W. (2006). A comparison of micro CT with other techniques used in the characterization of scaffolds. *Biomaterials,* 27, 8 (Mar 2006), 1362–1376, 0142-9612.

Hollister, S.J.; Fyhrie, D.P.; Jepsen, K.J. & Goldstein, S.A. (1991). Application of homogenization theory to the study of trabecular bone mechanics. *Journal of biomechanics*, 24, 9, 825–839, 0021-9290.

Hollister, S.J. & Kikuchi, N. (1992). A comparison of homogenization theory and standard mechanics analyses for periodic porous composites. *Computational Mechanics,* 10, 2 (Mar 1992), 73–95, 0178-7675.

Horbett, T.A.; Schway, M.B. & Ratner, B.D. (1985). Hydrophilic-hydrophobic copolymers as cell substrates-effect on 3T3 cell-growth rates. *Journal of colloid and interface science*, 104, 1 (Mar 1985), 28-39, 0021-9797.

Hutmacher, D.W. (2000). Scaffolds in tissue engineering bone and cartilage. *Biomaterials*, 21, 24 (Dec 2000), 2529-2543, 0142-9612.

Jaecques, S.V.N.; Van Oosterwyck, H.; Muraru, L.; Van Cleynenbreugel, T.; De Smet, E.; Wevers, M.; Naert, I. & Vander Floten, J. (2004). Individualised, micro CT-based finite element modelling as a tool for biomechanical analysis related to tissue engineering of bone. *Biomaterials,* 25, 9 (Apr 2004), 1683-1696, 0142-9612.

Lacroix, D.; Chateau, A.; Ginebra, M.P. & Planell, J.A. (2006). Micro-finite element models of bone-tissue engineering scaffolds. *Biomaterials,* 27, 30 (Oct 2006), 5326-5334, 0142-9612.

Langer, R. &Vacanti, J.P. (1993). Tissue Engineering. *Science,* 260, 5110 (May 1993), 920-926, 0193-4511.

Lorensen, W.E. & Cline, H.E. (1987). Marching Cubes: A high resolution 3D surface construction algorithm. *Computers & Graphics*, 21, 4 (July 1987), 163-169, 0097-8493.

Moroni, L.; de Wijn, J.R. & Blitterswijk, C.A. (2006). 3D fiber-deposited scaffolds for tissue engineering: Influence of pores geometry and architecture on dynamic mechanical properties. *Biomaterials,* 27, 7 (Mar 2006),974-985, 0142-9612.

Oliveira, S.M.; Mijares, D.Q.; Turner, G.; Amaral, I.F.; Barbosa, M.A. & Teixeira, C.C. (2009). Engineering endochondral bone: in vivo studies. *Tissue engineering. Part A*, 15, 3 (Mar 2009), 635-643, 1937-3341.

Otsu, N. (1979). A threshold selection method from gray-level histogram. *IEEE Transactions on Systems, Man, and Cybernetics*, 9, 1, 82-86, 1083-4427.

Mikos, A.G.; Sarakinos, G.; Leite, S.M.; Vacanti, J.P. & Langer, R. (1993). Laminated 3-dimensional biodegradable foams for use in tissue engineering. *Biomaterials*, 14, 5 (Apr 1993), 323-330, 0142-9612.

Parsons, J.R. (1985). Resorbable materials and composites. New concepts in orthopedic biomaterials. *Orthopedics,* 8, 7 (Jul 1985), 907–915, 0147-7447.

Rajan, G.P.; Fornaro, J.; Trentz, O. & Zellweger, R. (2006). Cancellous allograft versus autologous bone grafting for repair of comminuted distal radius fractures: a prospective, randomized trial. *The Journal of trauma,* 60, 6 (Jun 2006), 1322–1329, 0022-5282.

Thomson, R.C.; Wake, M.C.; Yaszemski, M. & Mikos, A.G. (1995). Biodegradable polymer scaffolds to regenerate organs. *Advances in Polymer Science*, 122, 1995, 247-274, 0065-3195.

van Lenthe, G.H.; Hagenmüller, H.; Bohner, M.; Hollister, S.J.; Meinel, L. & Müller, R. (2007). Nondestructive micro-computed tomography for biological imaging and quantification of scaffold–bone interaction in vivo. *Biomaterials*, 28, 15 (May 2007), 2749-2490, 0142-9612.

Whang, K.; Thomas, C.H.; Healy, K.E. & Nuber, G. (1995). A novel method to fabricate bioabsorbable scaffolds. *Polymer,* 36, 4 (Feb 1995), 837-842, 0032-3861.

Yang, S.; Leong, K.F.; Du, Z. & Chua, C.K. (2001). The design of scaffolds for use in tissue engineering. Part I. Traditional factors. *Tissue engineering*, 7, 6 (Dec 2001), 679–689, 1076-3279.

Zhang, R. & Ma P.X. (1999). Poly(alpha-hydroxyl acids)/hydroxyapatite porous composites for bone-tissue engineering. I. Preparation and morphology. *Journal of biomedical materials research*, 44, 4 (Mar 1999), 446-455, 0021-9304.

Zhou, Q.L.; Gong, Y.H. & Gao, C.Y. (2005). Microstructure and mechanical properties of poly(L-lactide) scaffolds fabricated by gelatin particle leaching method. *Journal of applied polymer science. Applied polymer symposium,* 98, 3 (Aug 2005), 1373-1379, 0271-9460.

Zienkiewicz, O.C.; Taylor, R.L. & Zhu, J.Z. (2006). *The finite element method, its basis & fundamentals.* 6th edition. Elsevier, Oxford, UK. 2006. 0750663200

IntechOpen

IntechOpen

Finite Element Analysis

Edited by David Moratal

ISBN 978-953-307-123-7

Hard cover, 688 pages

Publisher Sciyo

Published online 17, August, 2010

Published in print edition August, 2010

Finite element analysis is an engineering method for the numerical analysis of complex structures. This book provides a bird's eye view on this very broad matter through 27 original and innovative research studies exhibiting various investigation directions. Through its chapters the reader will have access to works related to Biomedical Engineering, Materials Engineering, Process Analysis and Civil Engineering. The text is addressed not only to researchers, but also to professional engineers, engineering lecturers and students seeking to gain a better understanding of where Finite Element Analysis stands today.

How to reference

In order to correctly reference this scholarly work, feel free to copy and paste the following:

Angel Alberich-Bayarri, Manuel Salmeron-Sanchez, M. Angeles Perez and David Moratal (2010). Microfinite Element Modeling for Evaluating Polymer Scaffolds Architecture and their Mechanical Properties from microComputed Tomography, Finite Element Analysis, David Moratal (Ed.), ISBN: 978-953-307-123-7, InTech, Available from: http://www.intechopen.com/books/finite-element-analysis/microfinite-element-modeling-for-evaluating-polymer-scaffolds-architecture-and-their-mechanical-prop

INTECH
open science | open minds

InTech Europe
University Campus STeP Ri
Slavka Krautzeka 83/A
51000 Rijeka, Croatia
Phone: +385 (51) 770 447
Fax: +385 (51) 686 166
www.intechopen.com

InTech China
Unit 405, Office Block, Hotel Equatorial Shanghai
No.65, Yan An Road (West), Shanghai, 200040, China
中国上海市延安西路65号上海国际贵都大饭店办公楼405单元
Phone: +86-21-62489820
Fax: +86-21-62489821

© 2010 The Author(s). Licensee IntechOpen. This chapter is distributed under the terms of the Creative Commons Attribution-NonCommercial-ShareAlike-3.0 License, which permits use, distribution and reproduction for non-commercial purposes, provided the original is properly cited and derivative works building on this content are distributed under the same license.

IntechOpen

IntechOpen